Feasibility of Ferumoxytol-Enhanced Neonatal and Young Infant Cardiac MRI Without General Anesthesia

Lillian M. Lai, MD,[1†] Joseph Y. Cheng, PhD,[1†] Marcus T. Alley, PhD,[1] Tao Zhang, PhD,[1] Michael Lustig, PhD,[2] and Shreyas S. Vasanawala, MD, PhD[1*]

Purpose: To assess the feasibility of ferumoxytol-enhanced anesthesia-free cardiac MRI in neonates and young infants for complex congenital heart disease (CHD).

Materials and Methods: With Institutional Review Board approval, 21 consecutive neonates and young infants (1 day to 11 weeks old; median age of 3 days) who underwent a rapid two-sequence (MR angiography [MRA] and four-dimensional [4D] flow) MRI protocol with intravenous ferumoxytol without sedation (n = 17) or light sedation (n = 4) at 3 Tesla (T) (except one case at 1.5T) between June 2014 and February 2016 were retrospectively identified. Medical records were reviewed for indication, any complications, if further diagnostic imaging was performed after MRI, and surgical findings. Two radiologists scored the images in two sessions on a 5-point scale for overall image quality and delineation of various anatomical structures. Confidence interval of proportions for likelihood of requiring additional diagnostic imaging after MRI was determined. For the possibility of reducing the protocol to a single rapid sequence, Wilcoxon-rank sum test was used to assess whether 4D flow and MRA significantly differed in anatomical delineation.

Results: One of 21 patients (4.8%, 80% confidence interval 0–11%) required additional imaging, a computed tomography angiography to assess lung parenchyma and peripheral pulmonary arteries. Only 1 of 13 patients (7.7%) with operative confirmation had a minor discrepancy between radiology and operative reports (80% confidence interval 0–17%). 4D flow was significantly superior to MRA ($P < 0.05$) for the evaluation of systemic arteries, valves, ventricular trabeculae, and overall quality. Using Cohen's kappa coefficient, there was good interobserver agreement for the evaluation of systemic arteries by 4D flow ($\kappa = 0.782$), and systemic veins and pulmonary arteries by MRA ($\kappa > 0.6$). Overall 4D flow measurements (mean $\kappa = 0.64$–0.74) had better internal agreement compared with MRA (mean $\kappa = 0.30$–0.64).

Conclusion: Ferumoxytol-enhanced cardiac MRI, without anesthesia, is feasible for the evaluation of complex CHD in neonates and young infants, with a low likelihood of need for additional diagnostic studies. The decreased risk by avoiding anesthesia must be balanced against the potential for adverse reactions with ferumoxytol.

Level of Evidence: 2

J. MAGN. RESON. IMAGING 2016;00:000–000

Cardiac MRI is an established modality for evaluation of congenital heart disease (CHD).[1,2] However, general anesthesia or deep sedation is typically used for complex congenital cardiac MR,[1,3] leading to decreased access, additional cost, and higher risk. With new free-breathing MR techniques with high spatial and temporal resolution, including four-dimensional (4D) flow,[4,5] and the use of ferumoxytol, with a long intravascular half-life, cardiac MR without sedation may be possible.

Ferumoxytol (Feraheme; AMAG Pharmaceuticals, Waltham, MA) is an ultra-small superparamagnetic iron oxide (USPIO) nanoparticle approved for the treatment of iron deficiency anemia in adults with chronic kidney disease, but off-label uses as an MRI contrast agent have been reported due to its excellent intravascular half-life of approximately 15 h, compared with 29 min for gadofosveset trisodium (Ablavar).[6,7] In patients with renal failure, ferumoxytol may serve as an alternative to gadolinium-based agents, without

View this article online at wileyonlinelibrary.com. DOI: 10.1002/jmri.25482

Received Mar 4, 2016, Accepted for publication Sep 1, 2016.

[†]Drs. Lai and Cheng contributed equally to this work.

*Address reprint requests to: S.S.V., 725 Welch Road St 1679 MC 5913, Palo Alto, CA 94304. E-mail: vasanawala@stanford.edu

From the [1]Department of Radiology, Stanford University, Stanford, California, USA; and [2]Department of Electrical Engineering and Computer Sciences, University of California, Berkeley, California, USA

Additional supporting information may be found in the online version of this article

the risk of developing nephrogenic systemic fibrosis. Ferumoxytol has been used for cardiac MRI. The long blood pool residence time of ferumoxytol as well as the marked signal enhancement in the blood pool permits free-breathing exams with high signal-to-noise ratio and reduced artifacts.[7]

Over the past few years, there has been increasing evidence of the risks of neurotoxicity from anesthesia.[8–11] These risks are thought to be highest in the newborn period and infancy and increased by longer duration of and greater cumulative exposure to anesthesia.[11] Thus, we have endeavored to leverage ferumoxytol's long intravascular half-life to reduce anesthesia depth, duration, and frequency. Ferumoxytol can be administered hours before the actual MRI exam. The patient can then be swaddled and possibly fed for the MRI scan. Also, in the event that an infant becomes uncooperative, imaging can simply be repeated when the infant is calm.

The major potential risk with ferumoxytol is a serious and potentially fatal hypersensitivity reaction, including anaphylaxis and hypotension, which has prompted an updated FDA black-box warning in March 2015.[12] However, the risks of ferumoxytol have to be considered in the full context of its potential advantages, including improved diagnostic evaluation and reduced anesthesia. General anesthesia has its inherent risks, including aspiration and respiratory compromise[13–17] in addition to the above described potential detrimental neurocognitive effects.[8–11]

For the past 2 years, we have used ferumoxytol for pediatric cardiovascular imaging with the approval of our institution's pharmacy committee, and obtained re-approval of that committee after the March 2015 FDA warning.[12] The aim of this study is to evaluate the feasibility of ferumoxytol-enhanced anesthesia-free cardiac MRI with a rapid two-sequence protocol in the evaluation of complex CHD in neonates and young infants.

Materials and Methods

With Institutional Review Board approval, Health Insurance Portability and Accountability Act compliance, and waived consent, we retrospectively identified 21 consecutive neonates and young infants (1 day to 11 weeks old, median age of 3 days, mean weight 3.3 ± 0.4 kg) who underwent a rapid, free-breathing, two sequence MRI protocol with intravenous ferumoxytol without any sedation ($n = 17$) or light sedation as needed with lorazepam or ketamine ($n = 4$) between June 2014 and February 2016 for CHD (Table 1). All patients received echocardiograms before cardiac MR.

Patients were intravenously injected with ferumoxytol 0–3.8 h (mean ± standard deviation : 1.3 ± 1.2) before imaging. Ferumoxytol was administered using a diluted volume in normal saline (3 mg/kg with 1:5 dilution) as a slow infusion over 5–15 min.[18] Vital signs were monitored for 30 min after administration with a physician with ACLS/PALS certification in the Radiology department or in the in-patient units. The patients were then fed, if possible, and bundled just before the MRI.

Patients were scanned on a 3 Tesla (T) ($n = 20$) or 1.5T ($n = 1$) MRI scanner (MR 750 3T and MR 450 1.5T; GE Healthcare, Waukesha, WI). The sole 1.5T case was due to lack of timely availability of the 3T scanner.

An axial MR angiography (MRA) was performed with an RF and gradient spoiled gradient echo sequence with fat-suppression followed by an axial volumetric time-resolved phase contrast acquisition (4D flow). The 4D flow acquisition was accelerated using parallel imaging and compressed sensing[5] It was also self-navigated. Field of view and slice thickness were adjusted to patients' size and weight. Imaging parameters are listed in Table 2. For both 4D flow and MRA, slices were reconstructed with 50% overlap, such that the interval between slices is half that of the slice thickness to facilitate multi-planar viewing. Average scan times were longer for 4D flow (8 min 55 s ± 2 min 21 s) compared with MRA (3–5 min). The majority of MRA images were obtained without cardiac triggering ($n = 17$). The remaining four cases were triggered to the diastolic phase, based on technologists' preference, which were accelerated using parallel imaging to achieve similar scan times as the nontriggered scans.

Two blinded, board-certified radiologists (first reader, L.M.L., with 4.5 years of MRI experience and second reader, S.S.V., with 13 years of MRI experience) independently scored the images on a five-point scale from 1 (nondiagnostic) to 5 (outstanding) for overall image quality and delineation of various anatomical structures on MRA and 4D flow. Overall image quality and delineation of systemic arteries, systemic veins, pulmonary arteries, pulmonary veins, heart valves, and ventricular trabeculae were evaluated according to predetermined criteria (Table 3). Details about the sittings and admixture of cases are described in Table 1. Medical records were reviewed for clinical indication, ferumoxytol dose, medications, complications, whether any further diagnostic imaging was performed after MRI (including catheterization), and operative confirmation of MRI findings.

Statistical Analysis

Confidence interval of proportions was calculated to assess the likelihood of requiring additional diagnostic imaging test after MRI and operative finding discordance. To evaluate the feasibility of reducing the protocol to a single 4D flow sequence, a Wilcoxon-rank sum score tested the null hypothesis that 4D flow was equivalent to MRA in quality of delineation of anatomical structures. Intraobserver and interobserver agreements were evaluated using weighted Cohen's Kappa (κ) coefficient. Kappa values were correlated to agreement as follows: less than chance (<0), slight (0.01–0.20), fair (0.21–0.40), moderate (0.41–0.60), substantial (0.61–0.80), and almost perfect (0.81–0.99) agreement.

Results

Salient clinical indications (Table 1) included potential vascular ring, arch hypoplasia or coarctation, double-outlet right ventricle, balanced atrioventricular canal, potential anomalous pulmonary veins, heterotaxy, tetralogy of Fallot, D-transposition, hypoplastic left heart, pulmonary vein stenosis, conotruncal abnormality, and connective tissue disorder. None of the patients had hypersensitivity reactions to

TABLE 1. Patient Demographics

Age (days)	Weight (kg)	Heart rate (bpm)	Time of contrast[a] (hours)	Clinical history/indication
2	3	136	0.0	Heterotaxy, AV canal, arch hypoplasia
3	3.57	126	0.0	Heterotaxy, arch hypoplasia
3	3	122	0.2	D-TGA, single coronary artery, pulmonic stenosis
6	3.14	151	0.6	Potential vascular ring
77	4.08	139	0.5	Heterotaxy with TAPVR
77	3.75	150	2.2	DORV with coarctation
1	2.54	127	3.8	Heterotaxy, DORV, AV canal, TAPVR
1	3.61	148	2.7	Hypoplastic left heart, TAPVR, coarctation
49	3.7	184	1.4	Potential pulmonary vein stenosis
6	3.5	118	0.2	Potential vascular ring
2	3.4	123	0.1	Heterotaxy, DORV, AV canal, TAPVR
1	3.56	147	0.3	Heterotaxy, DORV, AV canal, TAPVR, pulmonary stenosis
10	3.2	115	0.5	Tetralogy of Fallot with possible major aortopulmonary collaterals
2	3.43	154	2.6	Connective tissue disorder, evaluate aneurysms and coarctation
2	3.25	136	0.8	Truncus arteriosus
2	2.67	132	2.4	Potential vascular ring
15	3.68	146	0.8	Potential vascular ring
49	4.11	129	3.1	DORV with PAPVR
2	2.85	113	2.3	Potential vascular ring
6	2.76	158	0.3	Abnormal right pulmonary artery and diminished right ventricular function
4	3.3	116	2.0	Heterotaxy, AV canal, fetal bradycardia

[a]Time of contrast corresponds to the time between contrast administration and the MRI exam.
AV = atrioventricular; D-TGA = dextro-transposition of the great arteries; DORV = double outlet right ventricle; TAPVR = total anomalous pulmonary venous return; PAPVR = partial anomalous pulmonary venous return.

TABLE 2. MR Sequence Parameters

	4D Flow	MRA
TR (ms)	Minimum, 3.62-5.61	Minimum, 3.51-5.6
TE (ms)	Minimum, 1.62-2.54	Minimum, 0.75 – 2.11
Matrix	224 × 80 to 384 × 384	180 × 180 to 416 × 415
Slice thickness (mm)	0.7-2.4	0.5-2.4
Flip angle (degree)	12-20°, adjusted to stay within SAR limits	15°
Bandwidth (kHz)	62-100	83
Scan time (min:s)	8:50 ± 2:23	3-5 min
In-plane field of view (mm)	179 × 110 to 320 × 168	113 × 113 to 179 × 179
VENC (cm/s)	250	N/A

VENC = velocity encoding mapping sequence; SAR = specific absorption rate.

TABLE 3. Criteria for Scoring of Image Quality and Delineation of Anatomic Structures

Score	Overall image quality	Systemic arteries	Systemic veins	Pulmonary arteries	Pulmonary veins	Valves	Ventricles
5	Outstanding; answers all clinical questions; small arteries with high SNR and well-delineated	Both coronary artery origins well seen	Hepatic vein, IVC, SVC, azygous vein, and brachiocephalic vein all well seen (5/5)	Arteries within 1 cm of pleura	Can sharply see entrance to LA for all veins	Sharp on all phases (Not achievable on MRA since not cardiac gated).	Sharp trabeculae
4	Excellent; answers most clinical questions; medium arteries with high SNR and well-delineated	One coronary origin well seen	4/5 vessels well seen	All segmental arteries well seen	Can sharply see entrance to LA for some veins	Sharp	Trabeculae seen
3	Good; answers most important clinical questions; all medium arteries can be assessed	Arch vessels well seen	3/5 vessels well seen	Most segmental arteries well seen	Can see entrance to LA for all veins	Blurred	Sharp border
2	Poor but diagnostic; answers most important clinical question; all but 1-2 medium arteries assessed	Aorta well seen	2/5 vessels well seen	Lobar arteries well seen	Can see entrance to LA of some veins	Partially seen	Can perform segmentation
1	Non-diagnostic; does not answer clinical question; limited assessment of several medium arteries	Aorta not well seen	1/5 vessels well seen	Right and left pulmonary arteries well seen	Cannot see entrance to LA of some veins	Not seen	Cannot perform segmentation

SNR = signal-to-noise ratio; LA = left atrium; IVC = inferior vena cava; SVC = superior vena cava.

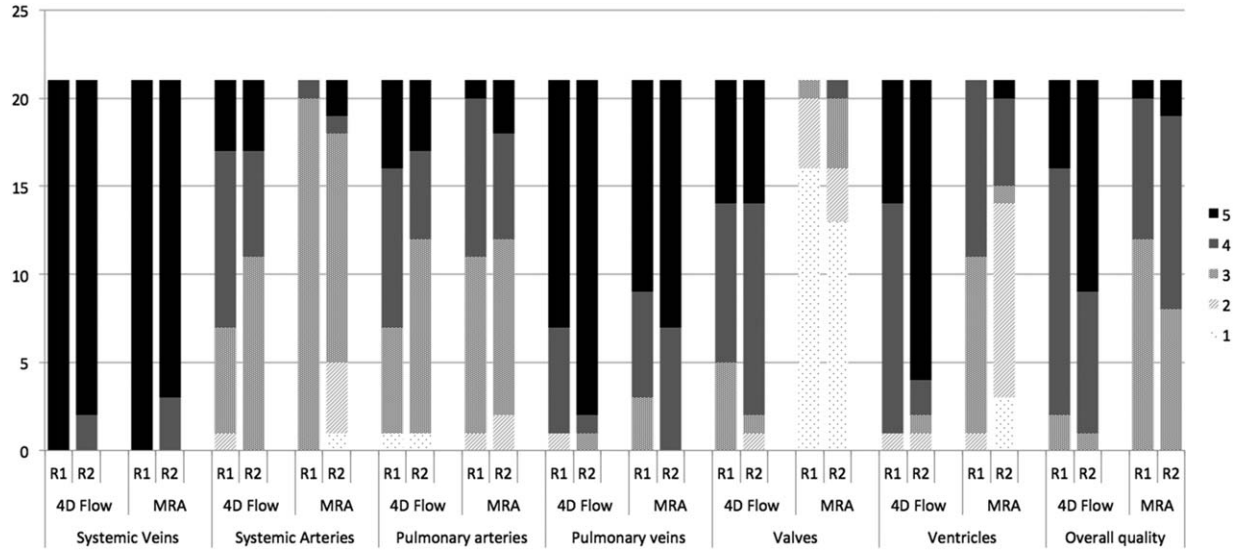

FIGURE 1: Performance of 4D flow and MRA in the delineation of various anatomical structures based on scores by the first reader (R1) and second reader (R2) over 21 studies, based on a scale from 1 (nondiagnostic) to 5 (outstanding). 4D flow was significantly superior to MRA for the evaluation of systemic arteries (inclusive of coronaries), valves, ventricular trabeculae, and overall quality (*$P < 0.05$). There was good interobserver agreement for the evaluation of systemic arteries by 4D flow ($\kappa = 0.782$), and systemic veins and pulmonary arteries by MRA ($\kappa > 0.6$). Overall 4D flow had better internal agreement compared with MRA.

ferumoxytol, nor needed any type of intervention related to ferumoxytol injection.

In terms of the diagnostic quality of ferumoxytol-enhanced cardiac MRI in neonates and infants and unresolved diagnostic questions, one patient was scanned at 1.5T (1/21, 4.8%), and was the only subject requiring additional imaging, a computed tomography angiography (CTA) performed largely to assess for lung parenchymal disease, but in part also for further delineation of peripheral pulmonary arteries. The 80% confidence interval of the proportion of exams requiring further imaging was thus up to 11%. Of 13 patients who underwent surgical repair, only 1 patient (7.7%) had a minor discrepancy between the radiology report and operative findings, with a small patent ductus arteriosus (PDA) seen at surgery but not on MRI (80% confidence interval up to 17%).

Time-resolved volumetric phase contrast (4D flow) was significantly superior to MRA for the delineation of systemic arteries (inclusive of coronary arteries), valves, ventricular trabeculae, and overall quality (Fig. 1). Similar mean scores for 4D flow and MRA, respectively, were observed for systemic veins (4.9 ± 0.3, 4.9 ± 0.3), pulmonary arteries (3.6 ± 1.0, 3.5 ± 0.7), and pulmonary veins (4.5 ± 0.7, 4.5 ± 0.6. Mean scores for 4D flow were significantly higher with $P < 0.005$ compared with MRA for systemic arteries (3.7 ± 0.8, 3.0 ± 0.6), valves (4.1 ± 0.8, 1.4 ± 0.7), ventricles (4.4 ± 0.7, 2.9 ± 1.2), and overall quality (4.2 ± 0.7, 3.6 ± 0.6). Even though MRA scans were acquired with either diastolic triggering or no diastolic triggering, we only observed a significant difference for the evaluation of valves where the images from the triggered scans were superior to nontriggered exams ($P < 0.05$ using a student t-test).

The readers had substantial interobserver agreement for the evaluation of systemic veins and pulmonary arteries by MRA ($\kappa > 0.64$), and systemic arteries by 4D flow ($\kappa = 0.78$). Lower interobserver agreement (slight to moderate) was observed for the analysis of valves (MRA: $\kappa = 0.41$, 4D flow: $\kappa = 0.25$), ventricles (MRA: $\kappa = 0.47$, 4D flow: $\kappa = 0.37$), pulmonary veins (MRA: $\kappa = 0.55$, 4D flow: $\kappa = 0.18$), and overall grade (MRA: $\kappa = 0.32$, 4D flow: $\kappa = 0.52$). There was not enough spread in the scoring for systemic veins to compute a meaningful kappa coefficient. Regardless, both readers rated 95.2% of cases as having a score of 4–5 for systemic veins reflecting our ability to obtain diagnostic image quality for these structures.

For intra-observer variability, there was moderate to near perfect agreement ($\kappa = 0.55$–0.86) for the evaluation of most anatomical structures by 4D flow for both readers, with the exception of systemic veins and pulmonary arteries ($\kappa < 0.24$) by the second reader. There was fair to poor intra-observer agreement ($\kappa = 0.17$–0.38) for the evaluation of systemic veins, pulmonary arteries, valves, and ventricles by MRA by the second reader and the evaluation of valves for both readers ($\kappa = 0.12$–0.38).

Figure 2 shows a representative example of the comprehensive evaluation of congenital heart disease. MR was able to delineate the complex anatomy in this patient before surgery, which included D-transposition, a single left main coming off single right coronary artery, and a PDA from right subclavian artery to the right pulmonary artery. The patient underwent arterial switch procedure with reimplantation of a single coronary button containing both coronaries, translocation of the right subclavian artery into the right common carotid artery, and PDA ligation.

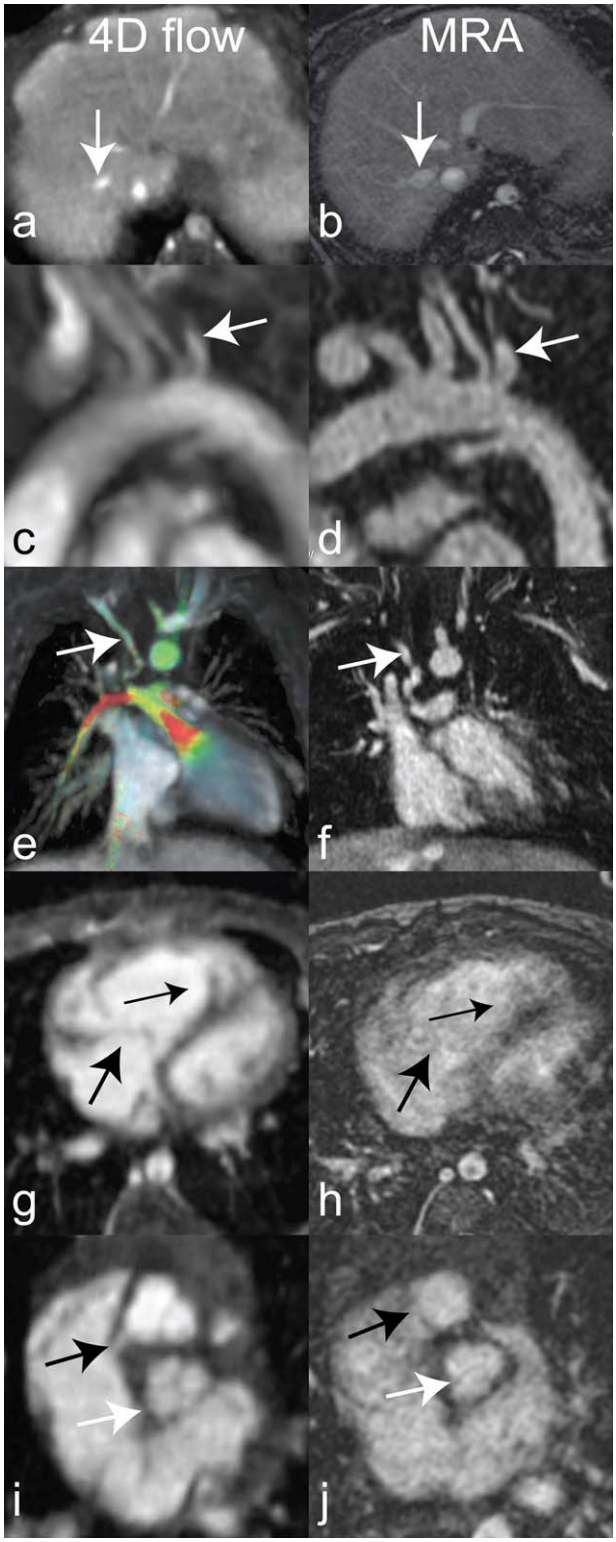

FIGURE 2: A 3-day-old male with D-transposition of great arteries and anomalous right subclavian artery from the right pulmonary artery. Structures are well delineated: hepatic veins (arrow) (a,b), arch vessels (arrow) (c,d), pulmonary arteries with anomalous right subclavian artery (arrow) (e,f), tricuspid valve (thick black arrow) and right ventricular trabeculae (thin black arrow) (g,h), and a single coronary artery (black arrows) (i,j), and trileaflet pulmonary valve (white arrows) (i,j).

Systemic arteries, such as the aorta, are well delineated. Figure 3 depicts aortic arch hypoplasia and aortic coarctation with increased velocities across the narrowing (1.54 m/s peak systolic velocity) and gradient of 10 mmHg, using 4D flow. The arch hypoplasia and coarctation were repaired by anastomosing the descending aorta to the aortic arch. Similarly, vascular rings are well-evaluated. Examples include a double aortic arch (Fig. 4a,b) that was revised, the PDA ligated, and the diverticulum of Kommerell was resected and explanted, and an asymptomatic right arch with aberrant left subclavian artery (Fig. 4c,d) that required no intervention. More complex great artery anomalies can also be assessed, as in Figure 5 (and Supplementary Videos S1-S4, which are available online) a truncus arteriosus with truncal valvular regurgitation, as well as a right pulmonary artery arising from a right-sided PDA. The truncus was repaired with a conduit to the reconstructed pulmonary arteries, and the PDA was ligated.

Another common indication was evaluation for anatomy of anomalous pulmonary venous return, as depicted in two separate cases of patients with heterotaxy, double outlet right ventricle (DORV), and total anomalous pulmonary venous return (TAPVR) (Fig. 6). Both TAPVRs were repaired, one also undergoing pulmonary artery (PA) banding and bidirectional Glenn (Fig. 6a,b) while the other (Fig. 6c,d) had a graft placed between the RV and the PA with atrial septectomy.

Intracardiac anatomy, including valves and ventricular trabeculae, was better depicted on 4D flow than MRA (Figs. 2–8). Figure 7 highlights the excellent depiction of valvular anatomy on 4D flow, which was found to be superior to MRA. This patient had a hypoplastic mitral valve with a single dominant papillary muscle, as well as DORV and partially anomalous pulmonary venous return (PAPVR), and is now status post bidirectional Glenn and repair of PAPVR. Similarly, Figure 8 highlights the ability of intracardiac anatomical evaluation in a patient with hypoplastic left heart and cor triatriatum, with good delineation of ventricular trabeculae, valve leaflets, and pulmonary venous drainage. The patient underwent Norwood procedure with RV to PA conduit and resection of cor triatriatum.

The Supplementary Videos S1-S4 show a 6-day-old male with hemitruncus, where the right pulmonary artery arose from the ascending aorta. The ratio of pulmonary flow to systemic blood flow (Qp:Qs) was more than 3, and the right to left pulmonary artery flow ratio was 6:1. There was evidence of increased right heart pressures (enlarged right atrium and ventricle) and markedly decreased right ventricular function with an ejection fraction of 13%. There was also pulmonary regurgitation (30%) and tricuspid regurgitation (70%). The potential of a rapid exam that can assess complex anatomy, quantify ventricular function, and also quantify blood flow is highlighted in this case, where

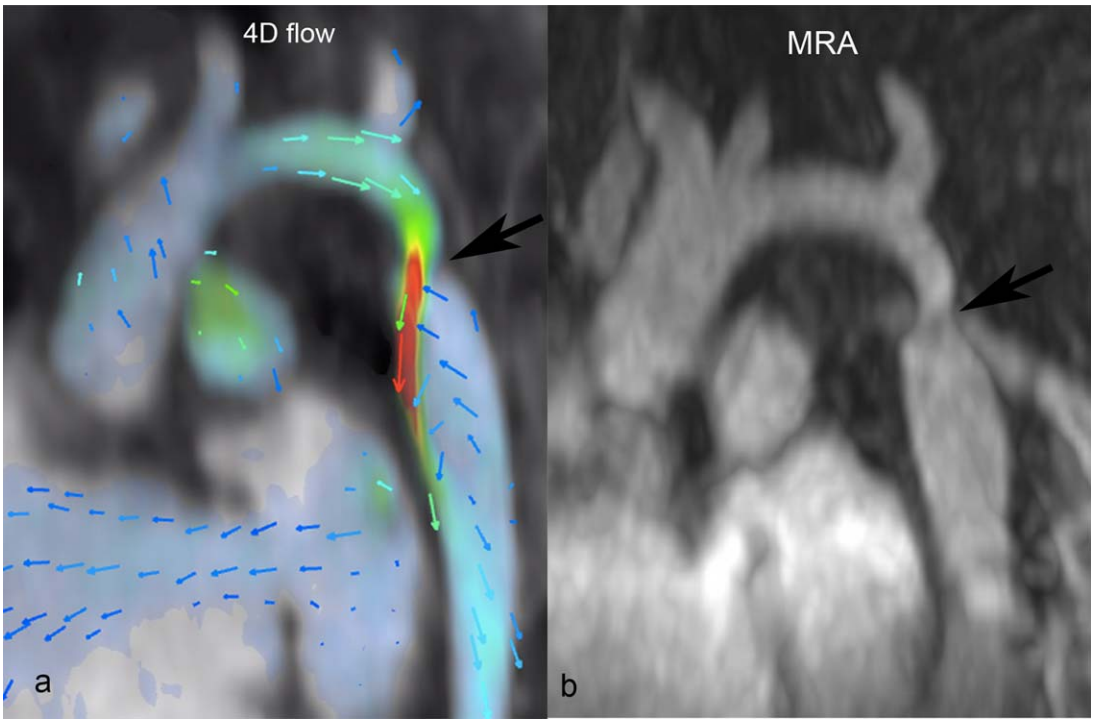

FIGURE 3: An 11-week-old male with double outlet right ventricle, hypoplastic arch, and aortic coarctation, as seen in 4D flow (left) and MRA (right) images, with a high flow velocity jet (black arrow). Peak systolic velocity at the coarctation was estimated at 1.54 m/s corresponding to a gradient of 10 mmHg.

the patient underwent repair of hemitruncus with LeCompte maneuver.

Discussion

We have shown that ferumoxytol-enhanced MRI without anesthesia is feasible for evaluation of complex CHD in neonates and young infants, with a low likelihood of need for additional diagnostic studies. With the long residence time of ferumoxytol in the blood pool, contrast can be administered well before the MRI and the infant be bundled and fed; if the child becomes agitated, re-imaging without need to inject another dose of contrast agent or compromise in image quality is possible. With iodine or gadolinium-based contrast agents, the resulting uncertainty of obtaining a concurrent period of patient cooperation and adequate contrast enhancement drives use of anesthesia. In this work, we combined the use of ferumoxytol with a rapid two-sequence protocol that includes a volumetric MRA and 4D flow. The MRA was performed without parallel imaging such that signal-to-noise ratio was increased and the artifacts from respiratory motion of free breathing were suppressed by signal averaging; diagnostic quality images were consistently obtained with minimal or no respiration artifacts in these neonates. Long scan times (3–5 min) for MRA without parallel imaging is enabled by the long blood pool residence time and long relaxivity of ferumoxytol. However, with these long scan times, voluntary motion is still an issue that limits depiction of small structures. Other motion correction strategies could be used to yield better MRA results, though that was not the focus of this work.

The 4D flow acquisition was accelerated and self-navigated. Because each of these sequences run for several minutes and benefitted from the long relaxivity of ferumoxytol, high-resolution images could be obtained to depict complex anatomy in small patients. Furthermore, because there was the chance the patient could wake up over these several minutes, the potential to repeat the scans afforded by ferumoxytol was critical. Three patients out of 20 (15%) were re-scanned, and all three scans then achieved diagnostic image quality.

4D flow was found to be superior to MRA in its ability to demonstrate valvular anatomy, ventricular trabeculae, and systemic arteries (inclusive of coronary arteries). This may be due in part to reduced cardiac motion artifacts from cardiac gating. Additionally, the ability to view the 4D flow images in cine clips enhanced our perception of the valves, trabeculae, and coronary arteries. Because 4D flow images were reconstructed in 20 min, whereas the MRA images were reconstructed immediately, MRA enables confidence in concluding the exam. To address this, the 4D flow sequence now acquires a low resolution, single echo set of *k*-space data at the beginning of the scan. This acquisition takes approximately 18 seconds, and the images can be reconstructed and returned to the scanner in under a minute while flow data are acquired. In addition to this, once the scan is completed we are able to perform a rapid

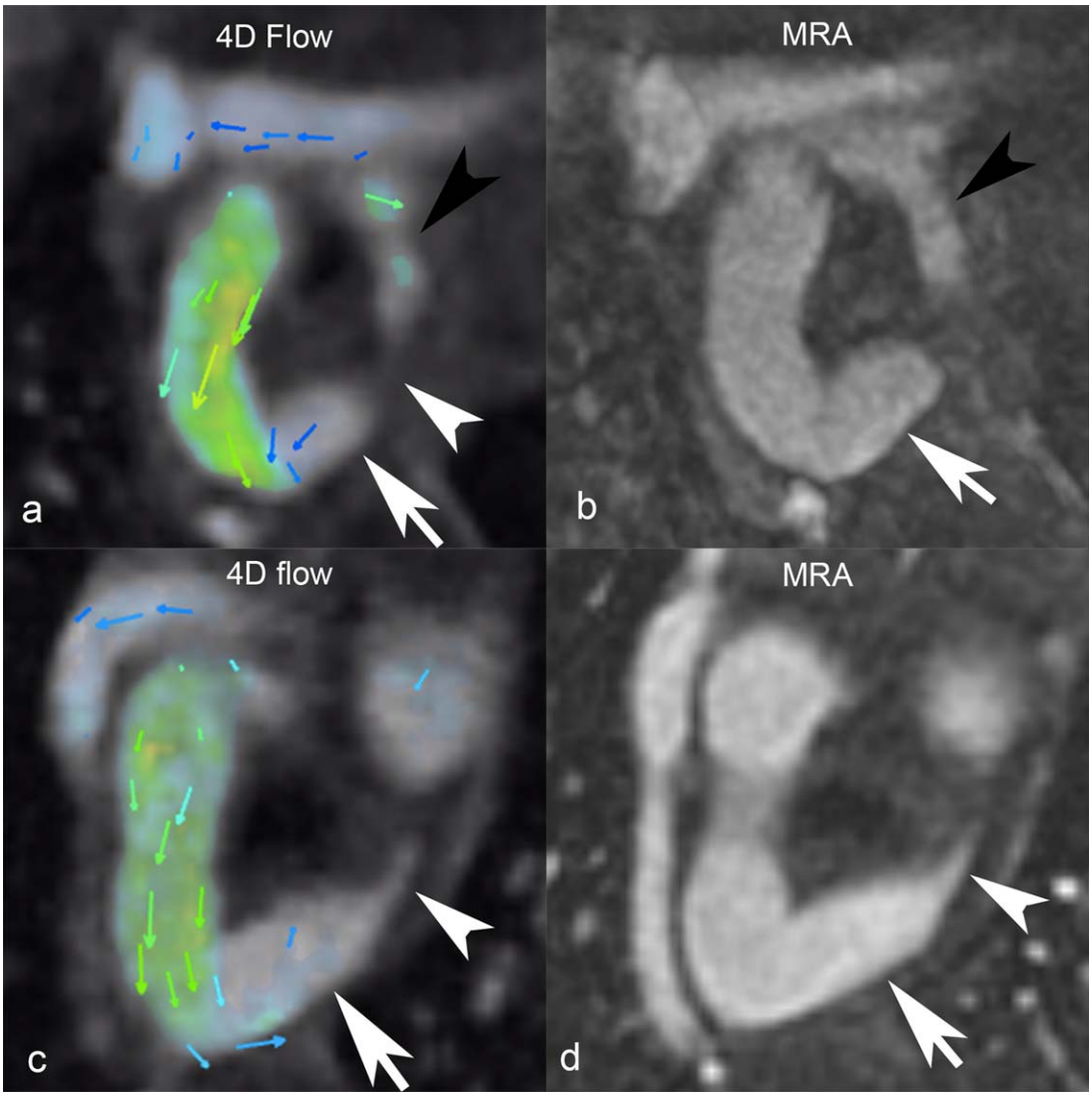

FIGURE 4: a,b: A 15-day-old male with right dominant double aortic arch with discontinuous left aortic arch (black arrowheads), left ductus arteriosus (white arrowhead), and large diverticulum of Kommerell (white arrows). c,d: A 2-day-old female with a right-sided aortic arch, aberrant left subclavian artery with small ductus arteriosus (white arrowheads), and large diverticulum of Kommerell (white arrows), creating a loose vascular ring.

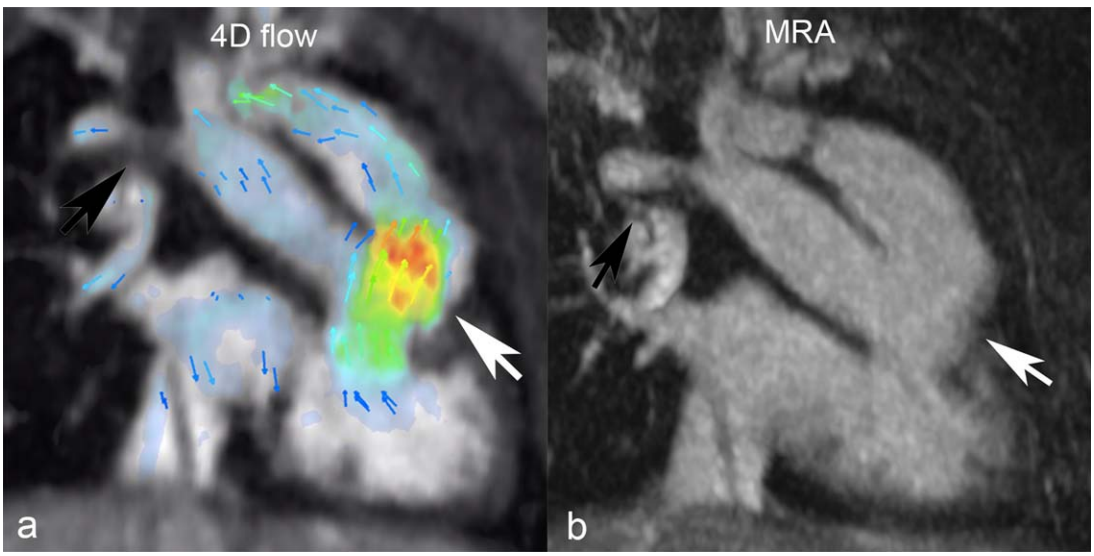

FIGURE 5: a,b: A 2-day-old male with truncus arteriosus (white arrows) and right-sided patent ductus arteriosus (black arrow).

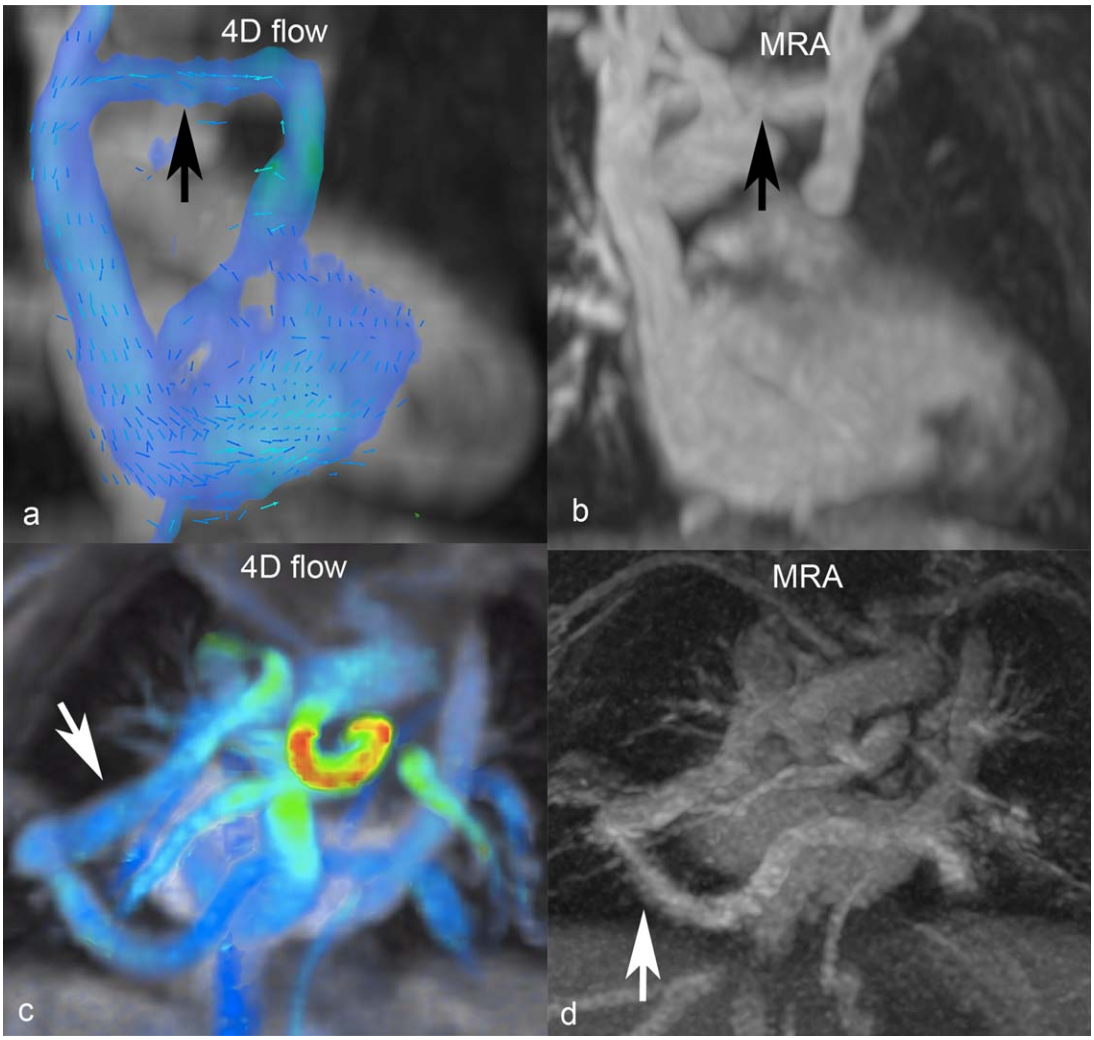

FIGURE 6: a,b: A 2-day-old male with heterotaxy, DORV, TAPVR (black arrows). c,d: A 1-day-old female with heterotaxy, DORV, and TAPVR (white arrows).

preliminary reconstruction from all cardiac phases of the 4D flow data using simple parallel imaging to effectively yield a nongated MRA after just several minutes.

There was excellent concordance between the radiology and operative reports. The only patient of 13 who had a minor discrepancy between the radiology report and surgical findings was scanned at 1.5T. In general 3T might be helpful for imaging small structures, but on the basis of one case, we cannot make any firm conclusions. Several noninvasive cardiac imaging techniques can serve to further

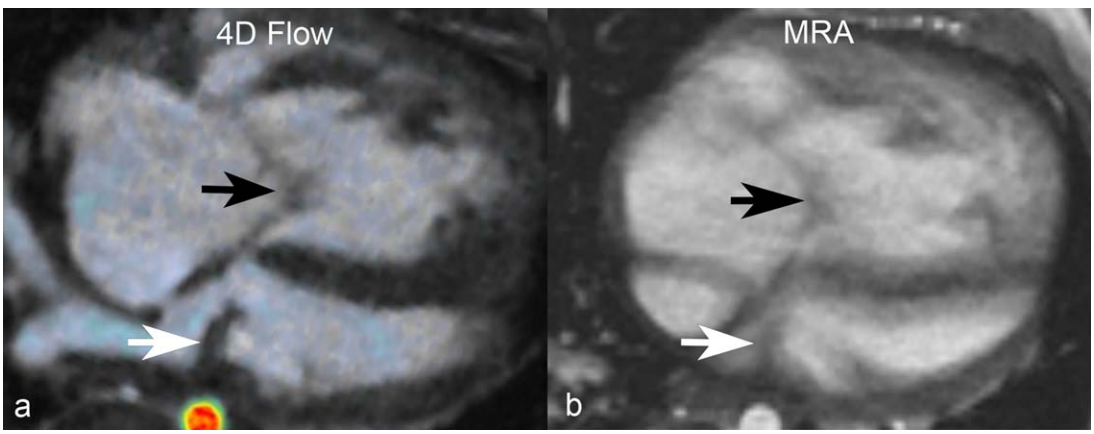

FIGURE 7: a,b: A 7-week-old female with DORV and PAPVR, with a normal tricuspid valve (black arrows) but a dysplastic mitral valve with thickened leaflet (white arrows).

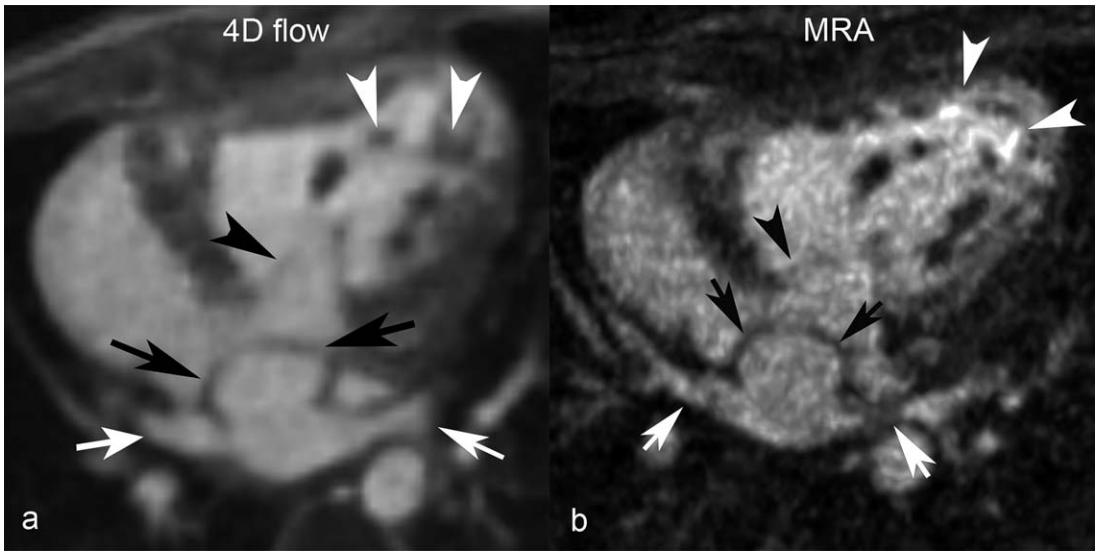

FIGURE 8: a,b: A 1-day-old male with hypoplastic left heart, TAPVR, and cor triatriatum, with an axial 4D flow magnitude image demonstrating right ventricular trabeculae (white arrowheads), tricuspid valve leaflets (black arrowheads), membrane of the cor triatriatum (black arrows), and pulmonary veins (white arrows).

diagnosis of CHD after echocardiography: CT angiogram with iodinated contrast, MRA with gadolinium-based agents, or MRA with ferumoxytol. The choice of modality involves several tradeoffs (Table 4). CT is faster, often has less motion artifacts, and can often better evaluate small structures like the coronary arteries without anesthesia, whereas MRI lacks ionizing radiation, has better cardiac temporal resolution, and quantifies flow and function.[2,3,19]

Ferumoxytol is not without risk, which should be weighed against the risks of anesthesia, performing additional potentially invasive studies, ionizing radiation, as well as the benefits of improved image quality and function/flow quantification without the physiologic perturbations of anesthesia. Since the FDA approval of ferumoxytol for therapy of iron deficiency in adults in 2009 and after more than 1.1 million distributed vials, 79 anaphylactic reactions and 18 fatalities despite immediate intervention have been documented after the administration of intravenous ferumoxytol.[12,20] In a large, multinational nonrandomized clinical trial, the reported rate of anaphylaxis was 0.02%.[21] In another trial the incidence of serious hypersensitivity reaction occurred in 0.2%, with hypotension occurring in 1.9% of patients.[22] Several smaller studies assessed the safety of ferumoxytol in children, though small sample sizes limit their significance.[20,23]

The incidence of immediate hypersensitivity reactions to gadolinium-based contrast agents was reported as 0.079%, with severe reactions including anaphylaxis occurring in 0.007% and a mortality rate of 0.0007%.[24] Other studies reported slight lower percentages of reactions to gadolinium-based agents. Prince et. al reported a mortality rate from anaphylaxis of 0.0019%,[25] and the FDA reported a mortality rate of 0.00008% from 2004 to 2009.[25] Thus, overall, the risk of serious hypersensitivity reactions is likely higher with ferumoxytol than gadolinium-based agents.

CT also has risks, including radiation and the risks of iodinated contrast. In one study, the estimated radiation dose in mSv for non-electrocardiography (ECG) gated cardiac CTAs for infants $\leq$3 kg was 0.42–1.29 mSv, and >3–6 kg was 1.28–1.61 mSv.[19] For ECG gated cardiac CTAs

TABLE 4. Tradeoffs between CTA, MRI, and MRI with Ferumoxytol

Modality	Benefits	Disadvantages
CTA with iodinated contrast	Fast imaging time	Possibly need for anesthesia Potential contrast nephropathy Ionizing radiation
MRI with gadolinium-based contrast	Lack of ionizing radiation Ventricular function and flow quantification	Need for anesthesia Nephrogenic systemic fibrosis Potential long-term gadolinium deposition
MRI with ferumoxytol contrast	Lack of ionizing radiation Anesthesia not necessary Simple comprehensive exam	Higher rate of anaphylaxis and hypotension compared with iodinated or gadolinium-based contrast agents

for children ≤10 years old, estimated radiation dose was 6.32 mSv.[19] With approximately 5% excess risk of fatal cancer per 1 Sv of radiation 26, As Low As Reasonably Achievable principles should be followed when imaging children.[3] Iodinated contrast can induce nephropathy as well as allergic reactions, including death (0.004%).[27] For children < 10 years old, prevalence of adverse contrast reactions was 0.4%.[27] Although neonatal CTA can often be performed without general anesthesia,[28] flow quantification cannot be obtained in this manner, and ventricular function assessment usually requires increased frequency of anesthesia and increased radiation dose.

Acute risks of sedation include respiratory, cardiovascular, and other events, which occurred in 534 per 10,000 anesthetic procedures using propofol.[13] In another study of 137 infants undergoing cardiac MRI with sedation, complications occurred in 5% of patients including one subject with a bradycardic event that prevented completion of exam and six other patients with transient vital sign changes that allowed exam completion.[2] Delayed risks with procedural sedation in children include delayed gastrointestinal complaints, restlessness and agitation, and motor imbalance.[14]

Anesthetic agents can be neurotoxic and can kill neurons in the developing brains of infantile animals including primates, though this cannot be directly tested in humans. However, anesthesia has been found to impair human brain function,[8] with decreased memory later in life after general anesthesia in infancy, independent of underlying disease.[9] Increased incidence of cognitive, developmental and behavioral disorders in children exposed to anesthesia have also been found.[10,11,15] Learning disabilities were more common in children who underwent more than one anesthetic and a longer cumulative anesthetic duration.[11] In another study, the risk of being diagnosed with developmental and behavioral disorders was 60% greater in children who had surgery with anesthesia when they were younger than 3 years old when compared with a similar matched group of siblings who did not have surgery/anesthesia.[15]

While general anesthesia is often required for full control of respiratory and physical motion,[16,17] the feed-and-sleep technique has been found to be well-tolerated, cost-efficient and safe in infants <6 months of age.[29] The scan times of those undergoing feed-and-sleep technique have been found to be generally similar to those undergoing general anesthesia or deep sedation.[17] In a 10-year institutional study, a review of safety of anesthesia in pediatric contrast angiography found that most adverse events (respiratory distress, bradycardia, etc.) were seen in patients undergoing general anesthesia and deep sedation, but not in the patients that only had "comforting measures."[17] Moreover, general anesthesia can induce changes in cardiac physiology and induce measurement errors in hemodynamically labile infants with complex CHD.[16]

One limitation of our study is the relatively small study size with our early experience with this technique and its retrospective nature. This limitation along with possible differences in interpretation of scoring criteria led to lower interobserver agreements for several anatomical structures. Another limitation is that direct comparison of image quality between ferumoxytol-enhanced MR angiography and other vascular imaging modalities (gadolinium-based blood pool agents, conventional angiography, etc.) has not been performed. However, studies in the past have shown ferumoxytol to be similar or superior in imaging quality to blood-pool gadolinium based agents[30] and consistent with results of other vascular tests including angiography.[31] Also, prior pediatric studies also have shown that qualitatively the vascular enhancement with ferumoxytol is greater than that of gadolinium-based agents.[7] Furthermore, based on our own extensive experience with gadofosveset trisodium (Ablavar), we have seen a significant decrease in blood pool enhancement 15 min after injection. Thus, we have not been confident enough to attempt anesthesia-free imaging of neonates with complex CHD with gadofosveset.

In conclusion, ferumoxytol-enhanced cardiac MRI without sedation or minimal sedation is feasible and provided excellent quality images to answer clinical diagnostic questions, with little likelihood for needing additional invasive imaging studies.

Acknowledgments

Contract grant sponsor: NIH; contract grant number: R01EB009690; Contract grant sponsor: NIH; contract grant number: R019241; Contract grant sponsor: GE Healthcare; Contract grant sponsor: Tashia and John Morgridge Faculty Scholar Fund

References

1. Kellenberger CJ, Yoo S-J, Büchel ERV. Cardiovascular MR imaging in neonates and infants with congenital heart disease. Radiographics 2007;27:5–18.
2. Johnson JT, Molina KM, McFadden M, Minich LL, Menon SC. Yield of cardiac magnetic resonance imaging as an adjunct to echocardiography in young infants with congenital heart disease. Pediatr Cardiol 2014;35:1067–1071.
3. Chan FP. MR and CT imaging of the pediatric patient with structural heart disease. Semin Thorac Cardiovasc Surg 2008;20:393–399.
4. Vasanawala SS, Hanneman K, Alley MT, Hsiao A. Congenital heart disease assessment with 4D flow MRI. J Magn Reson Imaging 2015;42: 870–886.
5. Cheng JY, Hanneman K, Zhang T, et al. Comprehensive motion-compensated highly-accelerated 4D flow MRI with ferumoxytol enhancement for pediatric congenital heart disease. J Magn Reson Imaging 2016;6:1355–1368.
6. Hartmann M, Wiethoff AJ, Hentrich HR, Rohrer M. Initial imaging recommendations for Vasovist angiography. Eur Radiol 2006:16(Suppl 2): B15–B23.

7. Rangamani S, Varghese J, Li L, et al. Safety of cardiac magnetic resonance and contrast angiography for neonates and small infants: a 10-year single-institution experience. Pediatr Radiol 2012;42:1339–1346.
8. Stratmann G. Review article: neurotoxicity of anesthetic drugs in the developing brain. Anesth Analg 2011;113:1170–1179.
9. Stratmann G, Lee J, Sall JW, et al. Effect of general anesthesia in infancy on long-term recognition memory in humans and rats. Neuropsychopharmacology 2014;39:2275–2287.
10. Rappaport B, Mellon RD, Simone A, Woodcock J. Defining safe use of anesthesia in children. N Engl J Med 2011;364:1387–1390.
11. Wilder RT, Flick RP, Sprung J, et al. Early exposure to anesthesia and learning disabilities in a population-based birth cohort. Anesthesiology 2009;110:796–804.
12. FDA Announcement: FDA strengthens warnings and changes prescribing instructions to decrease the risk of serious allergic reactions with anemia drug feraheme (ferumoxytol). Available at: http://www.fda.gov/Drugs/DrugSafety/ucm440138.htm. Accessed September 18, 2016.
13. Kiringoda R, Thurm AE, Hirschtritt ME, et al. Risks of propofol sedation/anesthesia for imaging studies in pediatric research. Arch Pediatr Adolesc Med 2010;164:554–560.
14. Schmidt MH, Marshall J, Downie J, et al. Pediatric magnetic resonance research and the minimal-risk standard. IRB 2011;33:1–6.
15. DiMaggio C, Sun LS, Li G. Early childhood exposure to anesthesia and risk of developmental and behavioral disorders in a sibling birth cohort. Anesth Analg 2011;113:1143–1151.
16. Dorfman A, Odegard K, Powell A, Laussen P, Geva T. Risk factors for adverse events during cardiovascular magnetic resonance in congenital heart disease. J Cardiovasc Magn Reson 2007;9:793–798.
17. Rangamani S, Varghese J, Li L, et al. Safety of cardiac magnetic resonance and contrast angiography for neonates and small infants: a 10-year single-institution experience. Pediatr Radiol 2012;42:1339–1346.
18. Vasanawala SS, Nguyen K-L, Hope MD, et al. Safety and technique of ferumoxytol administration for MRI. Magn Reson Med 2016;75:2107–2111.
19. Siripornpitak S, Pornkul R, Khowsathit P, Layangool T, Promphan W, Pongpanich B. Cardiac CT angiography in children with congenital heart disease. Eur J Radiol 2013;82:1067–1082.
20. Muehe AM, Feng D, von Eyben R, et al. Safety report of ferumoxytol for magnetic resonance imaging in children and young adults. Invest Radiol 2016;51:221–227.
21. Schiller B, Bhat P, Sharma A. Safety and effectiveness of ferumoxytol in hemodialysis patients at 3 dialysis chains in the United States over a 12-month period. Clin Ther 2014;36:70–83.
22. Lu M, Cohen MH, Rieves D, Pazdur R. FDA report: ferumoxytol for intravenous iron therapy in adult patients with chronic kidney disease. Am J Hematol 2010;85:315–319.
23. Ning P, Zucker EJ, Wong P, Vasanawala SS. Hemodynamic safety and efficacy of ferumoxytol as an intravenous contrast agents in pediatric patients and young adults. Magn Reson Imaging 2016;34:152–158.
24. Jung J, Kang H, Kim M, et al. Reaction to Gadolinium-based. Radiology 2012;264:414–422.
25. Prince MR, Zhang H, Morris M, et al. Incidence of nephrogenic systemic fibrosis at two large medical centers. Radiology 2008;248:807–816.
26. Miglioretti DL, Johnson E, Williams A, et al. The use of computed tomography in pediatrics and the associated radiation exposure and estimated cancer risk. JAMA Pediatr 2013;167:700–707.
27. Katayama H, Yamaguchi K, Kozuka T, Takashima T, Seez P, Matsuura K. Adverse reactions to ionic and nonionic contrast media. A report from the Japanese Committee on the Safety of Contrast Media. Radiology 1990;175:621–628.
28. Han BK, Overman DM, Grant K, et al. Non-sedated, free breathing cardiac CT for evaluation of complex congenital heart disease in neonates. J Cardiovasc Comput Tomogr 2013;7:354–360.
29. Windram J, Grosse-Wortmann L, Shariat M, Greer ML, Crawford MW, Yoo SJ. Cardiovascular MRI without sedation or general anesthesia using a feed-and-sleep technique in neonates and infants. Pediatr Radiol 2012;42:183–187.
30. Bashir MR, Mody R, Neville A, et al. Retrospective assessment of the utility of an iron-based agent for contrast-enhanced magnetic resonance venography in patients with endstage renal diseases. J Magn Reson Imaging 2014;40:113–118.
31. Li W, Salanitri J, Tutton S, et al. Lower extremity deep venous thrombosis: evaluation with ferumoxytol-enhanced MR imaging and dual-contrast mechanism--preliminary experience. Radiology 2007;242:873–881.